Synthesis and ferroelectric properties of multiferroic BiFeO$_3$ nanotube arrays

X. Y. Zhang, C. W. Lai, X. Zhao, D. Y. Wang, and J. Y. Dai[a]

Department of Applied Physics, The Hong Kong Polytechnic University, Kowloon, Hong Kong, People's Republic of China

We report the synthesis and characterization of ordered multiferroic BiFeO$_3$ (BFO) nanotube arrays. BFO nanotubes with diameters of about 250 nm and lengths of about 6 μm were fabricated by means of a sol-gel method utilizing nanochannel alumina templates. After postannealing at 700 °C, the BFO nanotubes exhibited a polycrystalline microstructure, and x-ray diffraction and transmission electron microscopy study revealed that they are of a perovskite crystal structure. Significant ferroelectric and piezoelectric characteristics of BFO nanotubes have been demonstrated by means of piezoresponse force microscopy measurement. © *2005 American Institute of Physics.* [DOI: 10.1063/1.2076437]

The prospect of a new generation of random access memory technology to handle the growing demand for memory is pushing several research fronts in this area,[1–4] such as magnetic random access memory and ferroelectric random access memory. Magnetism is involved with the local spin of electrons, while ferroelectricity represents a cooperative phenomenon that relies on the interaction of neighboring permanent electric dipoles in a crystal lattice. These two phenomena can coexist in some unusual perovskite-type oxide materials including magnetic elements, such as BiFeO$_3$,[5–7] BiMnO$_3$,[8,9] and TbMnO$_3$,[10,11] termed multiferroics. Multiferroics have attracted much attention because of their promise in the realization of a new type of memory by a combination of ferroelectric and ferromagnetic properties. As the development of nanoscale electronics approaches a practical stage, it is quite natural to ask how the crystal structure and state of polarization are influenced by the shape and size of multiferroic materials. The synthesis of multiferroic nanostructures with a controllable size and shape is critical not only in new device application, such as high-density magnetically recorded ferroelectric memory, but also from a fundamental point of view.

BiFeO$_3$ (BFO) is known to have rhombohedrally distorted perovskite structure. The space group R3c of BFO allows for a ferroelectric atomic displacement of below 1083 K and a weak ferromagnetism of below a Néel temperature T_N of 643 K simultaneously. The enhancement of polarization and related properties in heteroepitaxially constrained BFO films with a thickness of 200 nm has been reported. The films display a room-temperature spontaneous polarization almost of an order of magnitude higher than that of the bulk.[3,12] More recently, a giant ferroelectric polarization of beyond 150 μC/cm^2 has been obtained in BFO thin film deposited on a Pt/TiO$_2$/SiO$_2$/Si substrate at 90 K.[13] Ordered BFO nanostructure arrays are of considerable interest for future applications, such as a vertical magnetic recording with an ultrahigh recording density. In this letter, we report the synthesis of the BFO nanotube arrays by using a sol-gel template method. Significant ferroelectric and piezo-

electric characteristics of the BFO nanotube arrays have been revealed.

Nanochannel alumina (NCA) templates were prepared by means of anodization.[14,15] High-purity (99.999%) aluminum foils were used as the start material. Prior to anodizing, the aluminum was annealed at 500 °C in order to obtain homogeneous conditions for the growth of pores over large areas. Subsequently, the foils were electropolished in a 1:9 by volume mixture of HClO$_4$ and C$_2$H$_5$OH. Anodization was carried out for 12 h under a constant cell voltage of 180 V in a 0.3 M H$_3$PO$_4$ solution, and the temperature was kept constant at 0 °C. Then, the alumina was removed in a mixture of phosphoric acid and chromic acid, and the Al sheet was anodized again under the same condition as above. After the anodization, the remaining aluminum was removed in a saturated HgCl$_2$ solution. The pore bottoms were opened and widened by chemical etching in a 10% H$_3$PO$_4$ solution at 50 °C. The BFO nanotubes were synthesized by a sol-gel method utilizing the NCA templates. The BFO sol-gel precursor was prepared by dissolving bismuth nitrate Bi(NO$_3$)$_3$.5H$_2$O, and iron nitrate Fe(NO$_3$)$_3$.9H$_2$O in 2-methoxyethanol C$_3$H$_8$O$_2$, and followed by stirring for 30 min at room temperature. The concentration of the final solution was adjusted to 0.3 M with a pH value of 1–2 by adding 2-methoxyethanol and nitric acid. The NCA templates were immersed in the precursor solution for 20 min. In order to obtain the perovskite phase, the templates containing the precursor were subsequently heated in air at 700 °C for 60 min using a thermal annealing furnace. To measure the piezoelectric properties of the BFO nanotubes, the two surfaces of the BFO-filled NCA templates were mechanically polished to remove the BFO remaining on the surface until the BFO nanotubes emerged. A continuous Pt layer and dot electrodes with a thickness of about 100 nm were then coated on the two sides of the samples separately for dielectric and piezoelectric response characterizations. The structure and morphology of the BFO nanotubes were investigated using x-ray diffraction (XRD) (D/Max 2250V), a scanning electron microscope (SEM) (JEOL JSM-6300), and a high-resolution transmission electron microscope (HR-TEM) (JEOL-2010). The dielectric property was measured using a precision impedance analyzer (Agilent 4294A), and

---
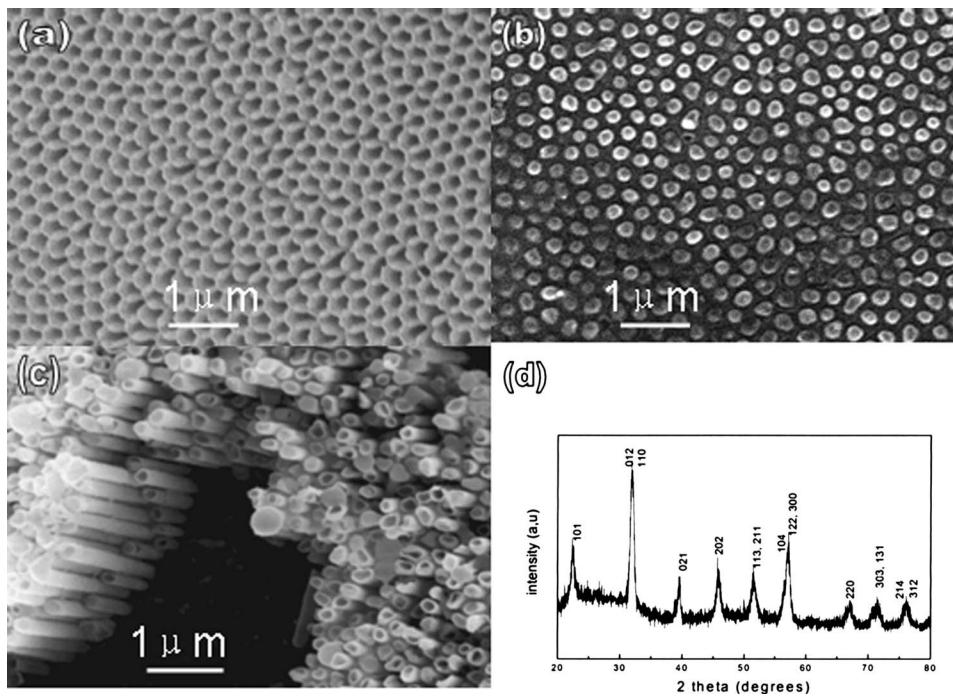[a]Electronic mail: apdaijy@inet.polyu.edu.hk

FIG. 1. SEM images of the nanochannel alumina (NCA) template and BFO nanotubes: (a) NCA template, (b) top view of the nanochannel porous alumina filled with BFO nanotubes, (c) oblique view of BFO nanotube arrays, and (d) XRD pattern of the BFO nanotube arrays.

the piezoelectric property of the BFO nanotubes was measured by piezoresponse force microscopy using a commercial scanning probe microscope (Nanoscope IV, Digital Instruments) equipped with a conductive tip and a lock-in amplifier (SR830, Stanford Research Systems).

Figures 1(a) and 1(b) show the SEM images of the closely packed porous NCA template and one filled with BFO nanotubes, respectively. The pore diameters and the thickness of the NCA template are about 250 nm and 6 μm, respectively; and it can be seen that almost all of the pores are filled with BFO nanotubes. Figure 1(c) is the corresponding SEM image of the free-standing BFO nanotube arrays after the alumina was etched away using a 4 M NaOH solution. The XRD spectrum of the BFO nanotubes after the alumina was dissolved away is shown in Fig. 1(d). The reflection peaks are clearly distinguishable, and can be perfectly indexed as a rhomohedrally distorted perovskite BFO structure. No obvious reflections that would indicate the existence of second phases were detected.

Figure 2(a) shows the transmission electron microscope (TEM) image of BFO nanotubes after the alumina was dissolved away; it is apparent that the BFO nanotubes are of a uniform diameter. Figure 2(b) shows the TEM image of a single BFO nanotube. The right-hand side inset shows the energy dispersive x-ray (EDX) spectrum taken from the in-

dividual nanotube, the nanotubes are composed of equal quantities of the elements Bi and Fe. The left-hand side inset shows the selected area electron diffraction pattern (SAED) taken from the nanotube, which reveals the polycrystalline structure nature of the BFO nanotubes. The perovskite structure of the BFO nanotubes was further confirmed by HR-TEM image as shown in Fig. 3. It can be seen that the BFO nanotubes are composed of nanoparticles of sizes ranging from several to ten nanometers, and that the average wall thickness of the nanotubes is about 20 nm. The well-recognized lattice spacing of 0.395 nm corresponds to the {101} atomic planes.

In order to demonstrate the ferroelectric characteristics of the BFO nanotubes, piezoresponse d_{33} hysteresis loop of an individual BFO nanotube was measured using the conductive atomic force microscope tip applied with a 16.5 kHz ac electric field plus a swept dc voltage, and the result is shown in Fig. 4. The details of the piezoresponse measurement have been reported earlier, where the piezoelectric properties of $Pb(Zr_{0.53}Ti_{0.47})O_3$ nanowires were studied.[16] The decrease in d_{33} at high electric field, as shown in Fig. 4,
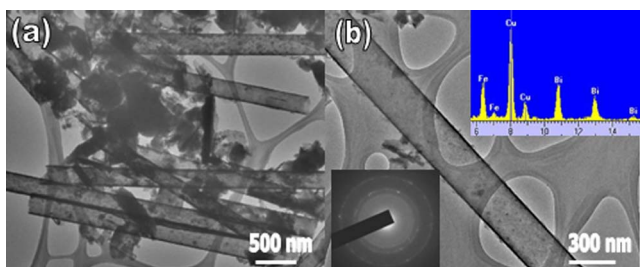

FIG. 2. (a) TEM image of the BFO nanotubes after completely dissolving the NCA template, and (b) TEM image of an isolated BFO nanotube, the left inset shows the corresponding SAED pattern, the right inset shows the EDX spectrum.
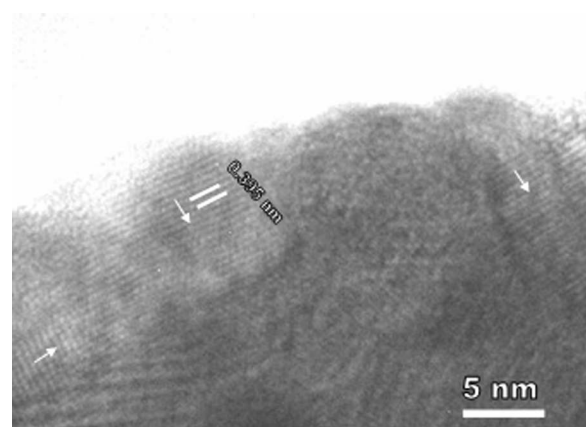

FIG. 3. HRTEM image of the BFO nanotubes, the arrows indicate the {101} atomic planes with lattice spacing around 0.395 nm.
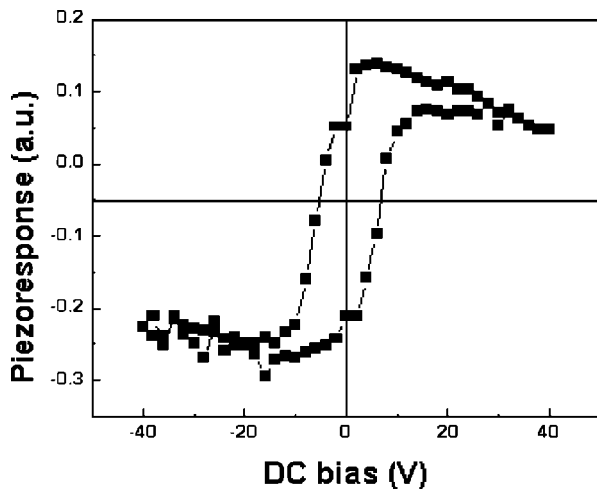
FIG. 4. Piezoelectric hysteresis loop of a single BFO nanotube measured by piezoresponse force microscopy.

is believed to be a consequence of the field-induced lattice hardening, which is typical for perovskite piezoelectrics.[4] The significant piezoelectric characteristics illustrate the ferroelectric behavior of the BFO nanotubes.

Figure 5 shows the dielectric constant and dielectric loss of the BFO nanotube arrays measured at room temperature as a function of frequencies in the range of 1 kHz to 1 MHz. Both the dielectric constant and the dielectric loss show a remarkable decrease of up to 10 kHz and remain fairly constant afterward. The decrease in the dielectric constant with an increase in frequency represents the anomalous dispersion
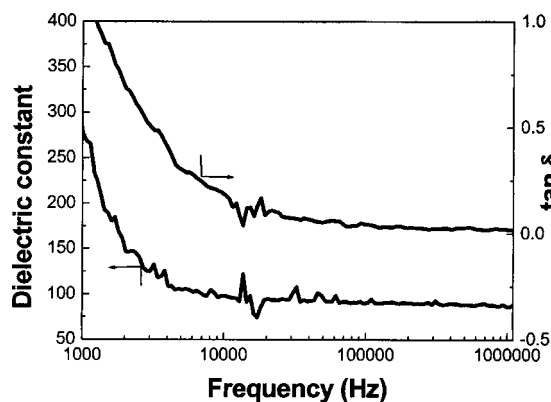

FIG. 5. The dielectric constant and dielectric loss curves at room temperature as a function of frequency in the range of 1 kHz to 1 MHz.

of the dielectric constant at low and intermediate frequencies, which has been explained by the phenomenon of dipole relaxation; while the variation in dielectric loss with frequency represents the relaxation absorption of the dielectric.[17] The dielectric constant and dielectric loss were 90 and 0.04, respectively, at 100 kHz. The dielectric constant value matches well with the values reported in the literature.[18,19]

In summary, ordered BFO nanotube arrays were fabricated using sol-gel synthesis within hexagonal closely packed nanochannel alumina templates. These BFO nanotube arrays exhibit significant piezoelectric characteristics and may have potential application in fabrication of magnetically recorded ferroelectric memory, and lead-free piezoelectrics for sensors and actuators.

[1] N. Hur, S. Park, P. A. Sharma, J. S. Ahn, S. Guha, and S. W. Cheong, Nature (London) **429**, 392 (2004).
[2] W. H. Butler and A. Gupta, Nat. Mater. **3**, 845 (2004).
[3] J. Wang, J. B. Neaton, H. Zeng, V. Nagarajan, S. B. Ogale, B. Liu, D. Viehland, V. Vaithyanathan, D. G. Schlom, U. V. Waghmare, N. A. Spaldin, K. M. Rabe, M. Wuttig, and R. Ramesh, Science **299**, 1719 (2003).
[4] H. Zeng, J. Wang, S. E. Lofland, Z. Ma, L. Mohaddes-Ardabill, T. Zhao, L. Salamanca-Riba, S. R. Shinde, S. B. Ogale, F. Bai, D. Viehland, Y. Jia, D. G. Schlom, M. Wuttig, A. Roytburd, and R. Ramesh, Science **303**, 661 (2004).
[5] M. M. Kumar and V. R. Palkar, Appl. Phys. Lett. **76**, 440 (2003).
[6] V. R. Palkar, J. John, and R. Pinto, Appl. Phys. Lett. **80**, 440 (2003).
[7] V. L. Mathe, K. K. Patankar, and R. N. Patil, J. Magn. Magn. Mater. **270**, 380 (2004).
[8] T. Kimura, S. Kawamoto, I. Yamada, M. Azuma, M. Takano, and Y. Tokura, Phys. Rev. B **67**, 180401 (2003).
[9] J. Y. Son, B. G. Kim, C. H. Kim, and J. H. Cho, Appl. Phys. Lett. **84**, 4971 (2004).
[10] T. Kimura, T. Goto, H. Shintani, K. Ishizaka, T. Arima, and Y. Tokura, Nature (London) **426**, 6962 (2003).
[11] I. O. Troyanchuk, N. V. Samsonenko, N. V. Kasper, H. Szymczak, and A. Nabialek, J. Phys.: Condens. Matter **9**, 8287 (1997).
[12] J. Wang, H. Zeng, Z. Ma, S. Prasertchoung, M. Wuttig, R. Droopad, J. Yu, K. Eisenbeiser, and R. Ramesh, Appl. Phys. Lett. **85**, 2574 (2004).
[13] K. Y. Yun, D. Ricinschi, T. Kanashima, M. Noda, and M. Okuyama, Jpn. J. Appl. Phys., Part 2 **43**, L647 (2004).
[14] H. Masuda and K. Fukuda, Science **268**, 1466 (1995).
[15] X. P. Hoyer and H. Masuda, J. Mater. Sci. Lett. **15**, 1228 (1996).
[16] X. Y. Zhang, X. Zhao, C. W. Lai, J. Wang, X. G. Tang, and J. Y. Dai, Appl. Phys. Lett. **85**, 4190 (2004).
[17] A. A. Zaky and R. Hawley, *Dielectric Solids* (Dover, New York, 1970).
[18] G. Teowee, K. McCarthy, F. McCarthy, T. J. Bukowski, T. P. Alexander, and D. R. Uhlmann, Integr. Ferroelectr. **18**, 329 (1997).
[19] K. Y. Yun, M. Noda, M. Okuyama, H. Saeki, H. Tabata, and K. Saito, J. Appl. Phys. **96**, 3399 (2004).